Indian Journal of Pure & Applied Physics
Vol. 43, July 2005, pp. 535-541

Electrical conductivity and thermoelectric power of $Ge_{40}Te_{60}$ and $Ge_{38}Sn_2Te_{60}$ alloys

A M Ahmed

Physics Department, Faculty of Science, South Valley University, 82524 Sohag, Egypt

Received 25 February 2004; revised 19 April 2004; accepted 16 May 2005

The *dc* conductivity (σ) and thermoelectric power (TEP) have been measured for the bulk binary alloy $Ge_{40}Te_{60}$ and ternary alloy $Ge_{38}Sn_2Te_{60}$. X-ray diffraction confirms that the samples are polycrystalline. The measurments were carried out in the temperature range $133 < T < 400$ K. Variation of electrical conductivity with ambient temperature (T) proved the semiconductor behaviour for all range of T for both materials. With annealing time (t_{an}), the electrical conduction activation energy (E_σ) has been found to be with range from 0.11×10^{-3} eV-63.3×10^{-3} eV for $Ge_{40}Te_{60}$ and from 0.95×10^{-3} to 52.93×10^{-3} eV while the thermo-electric power activation energy (E_s) has been found to be in the range 2.28×10^{-3}-39.3×10^{-3} eV and 1.58×10^{-3}-34.2×10^{-3} eV for two alloys, respectively.

Keywords: Elecrical conductivity, Thermo-electric power, Activation energy

IPC Code: G01R 21/08

1 Introduction

For several practical application reasons the IV-VI semiconducting compounds A^{IV} B^{VI} (A^{IV} = Ge, Sn, Pb; B^{VI} = S, Se, Te) have attained great interest and attention[1-5]. In addition, they also possess some unusual and possibly unique properties such as high dielectric constant and high carrier mobility as well as a narrow fundamental gap of several tenths of an electron volt at the *L* point. As a result of their narrow fundamental gap, the IV-VI semiconductors are suitable as infrared detectors and light emitting devices. Hence, their optical and electric properties both theoretically[6-9] and experimentally[10-12] have been studied.

Haruvi-Busnach *et al*.[4] have prepared chalcogenide glasses of the systems Ge-Sn-Se, Ge-Se-Te and Ge-Sn-Se-Te. They used X-ray diffraction, DSC (differential scanning calorimetry), SEM (scanning electron microscopy) with EDAX (energy dispersive analysis of X-ray) analysis, FTIR spectrometry to characterize the glasses. They found the glass transition temperature and microhardness of Ge-Sn-Se and Ge-Sn-Se-Te glasses decrease with increasing Sn content for most of the samples. The region of high IR transparency of Ge-Sn-Se, Ge-Se-Te and Ge-Sn-Se-Te glasses was slightly expanded (1-2 μm) towards longer wavelengths, compared to Ge-Se glasses, mainly for the glasses containing ≤ 70 % Se. The intensity of the impurity absorbtion peak Ge-O (at $\lambda \sim 12.8$ μm) which usually appears in Ge-Se glasses, was reduced or was absent in Ge-Sn-Se-Te glasses. The mechanical and optical characteristics of these glasses have been related to the glass structure.

Meaningful interpretation of the nature of electron transport is difficult without detailed *dc* conductivity studies. Thus, the effect of both the ambient temprature and the time of annealing on Seebeck coefficient and the electrical conductivity of $Ge_{40}Te_{60}$ and $Ge_{38}Sn_2Te_{60}$ alloys has been investigated.

2 Experimental Details

The two samples $Ge_{40}Te_{60}$ and $Ge_{38}Sn_2Te_{60}$ were prepared using the conventional melt-quench technique. Appropriate amount of high purity (99.99%) constituent elements were sealed in a quartz ampoule 8 mm diameter at about 10^{-3} pa. Alloying was performed at 900°C for 12 h. During alloying the ampoule was shaken rigorously several times to ensure thorough mixing of the constituents, and hence good homogeneity of the produced alloy. After that, the alloy was allowed to cool to 600°C in 6 h, and further cooled to 400°C also through 6 h.

Quenching was performed in ice cooled water. Bulk samples with parallel and optically flat surfaces were prepared by sawing using an automatic cutting machine with diamond saw. Polishing was performed

mechanically by means of a controlled velocity rotating disc. The measurements of the *dc* electrical conductivity were carried out using a pressure contact sample holder. The opposite parallel surfaces of a sample were painted with silver paste as contact electrodes. A conventional series current circuit was used. The current was measured by means of Keithley 175 digital multimeter (DMM), while the potential difference was measured by means of Keithley 177 microvolt DMM. The senstivity of measuring current and potential difference was 1×10^{-6} A and 1×10^{-6} V, respectively. A copper-constantan thermocouple junction was used for monitoring the temperature.

The thermoelectric power measurements were carried out using the simple two heaters method with graphite electrodes. The difference in temperature between the two opposite surfaces of the sample was 3°C during the whole measurements. The thermoelectric voltage was measured by means of Keithley 177 microvolt DMM. The X-ray diffractograms of the samples were studied using X-ray diffracotmeter type Philips (Holland) model PW 1710. The X-ray diffractograms shown in Figs 1 and 2, show that the prepared sample materials $Ge_{40}Te_{60}$ and $Ge_{38}Sn_2Te_{60}$ have polycrystalline structure. Figure 1 shows that the most intense peaks correspond to those of the original composition GeTe. In addition, the less intense peaks correspond to the elements Te and Ge. It was observed that the intensity of the most peaks increases by annealing. Further, the position of the especially most intense peak has been shifted towards higher diffraction angle with annealing.

Figure 2 shows that the most intense peaks correspond to the ternary composition GeSnTe. The other less intense peaks correspond to the binary phases GeTe and SnTe. In addition, the peaks for the elements Ge, Sn and Te could also be identified. In case of $Ge_{38}Sn_2Te_{60}$, the intensity of the most intense peak decreases due to annealing while still position of these peaks has been shifted towards higher diffraction angle.

3 Results and Discussion

The two samples $Ge_{40}Te_{60}$ and $Ge_{38}Sn_2Te_{60}$ were annealed isothermally at 200°C for different times (0, 40, 160, 640, 1280 minutes). The *dc* conductivity σ and Sebeck coefficient (*S*) were measrued after each period of annealing in the temperature range of $133<T<400$ K. Figures 3 and 4 show the variation of lnσ with $1/T$ for $Ge_{40}Te_{60}$ and $Ge_{38}Sn_2Te_{60}$, respectively. As shown in Figures 3 and 4, the plots corresponding to all periods of annealing at 200°C indicate two segments corresponding to two values of the activation energy. The temperature dependence is weak at lower temperatures confirming the domination of hopping conduction mechanism. Contrary to this, the temperature dependence becomes relatively stronger at higher temperatures which reveals the possibility of conduction due to extended state. Therefore, the temperature dependence of the electrical conductivity within this range can be described by the following usual Arrhenius equation

$$\sigma=\sigma_0\exp\left(-\frac{E_\sigma}{kT}\right) \quad \ldots (1)$$

where σ_0 is the conductivity pre-exponential factor and E_σ is the activation energy for conduction. The

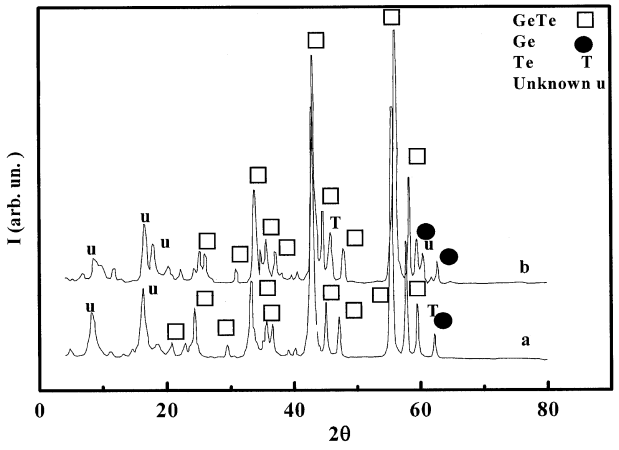

Fig. 1—X-ray diffractograms for $Ge_{40}Te_{60}$. (a) as prepared sample (b) annealed sample at 200°C for 1280 min

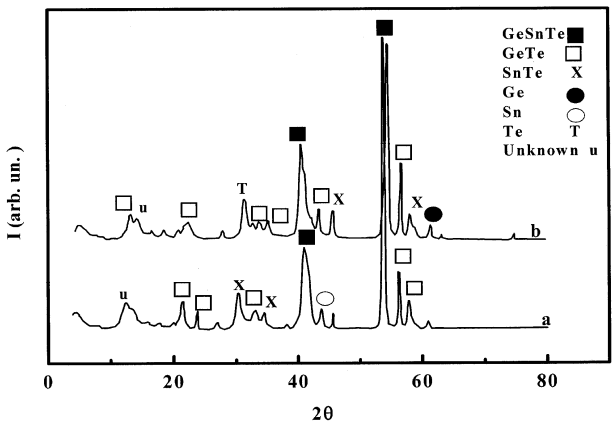

Fig. 2—X-ray diffractograms for $Ge_{38}Sn_2Te_{60}$. (a) as prepared sample (b) annealed sample at 200°C for 1280 min

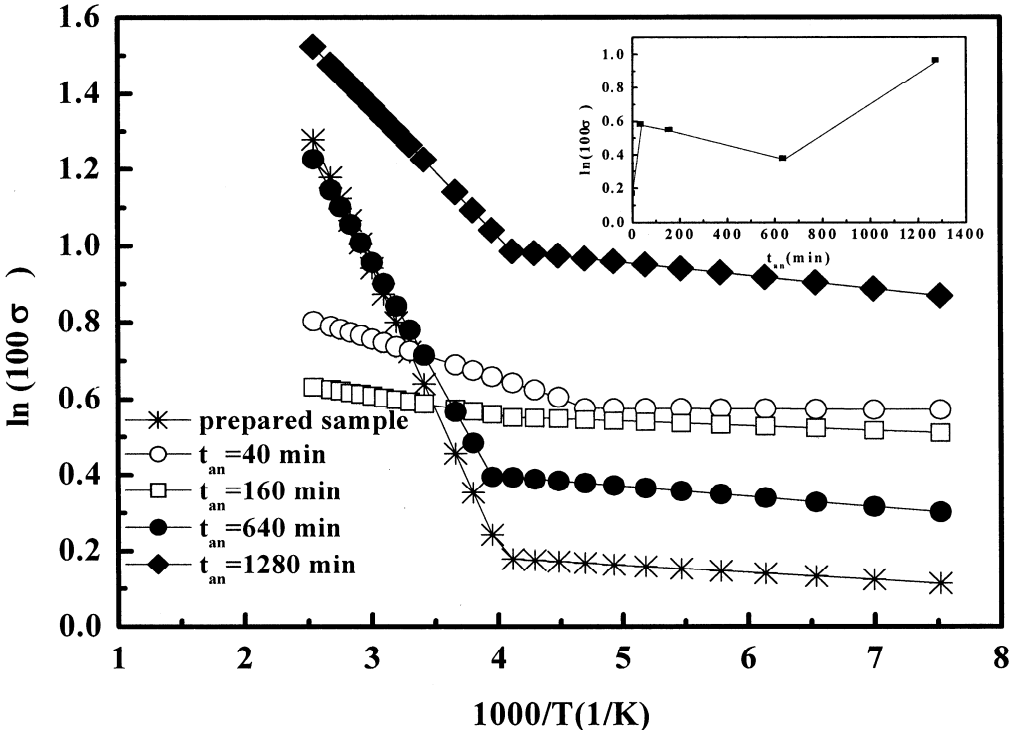

Fig. 3—Temperature dependence of conductivity at different annealing times for $Ge_{40}Te_{60}$. The inset shows the dependence of conductivity on annealing time at T=200°C

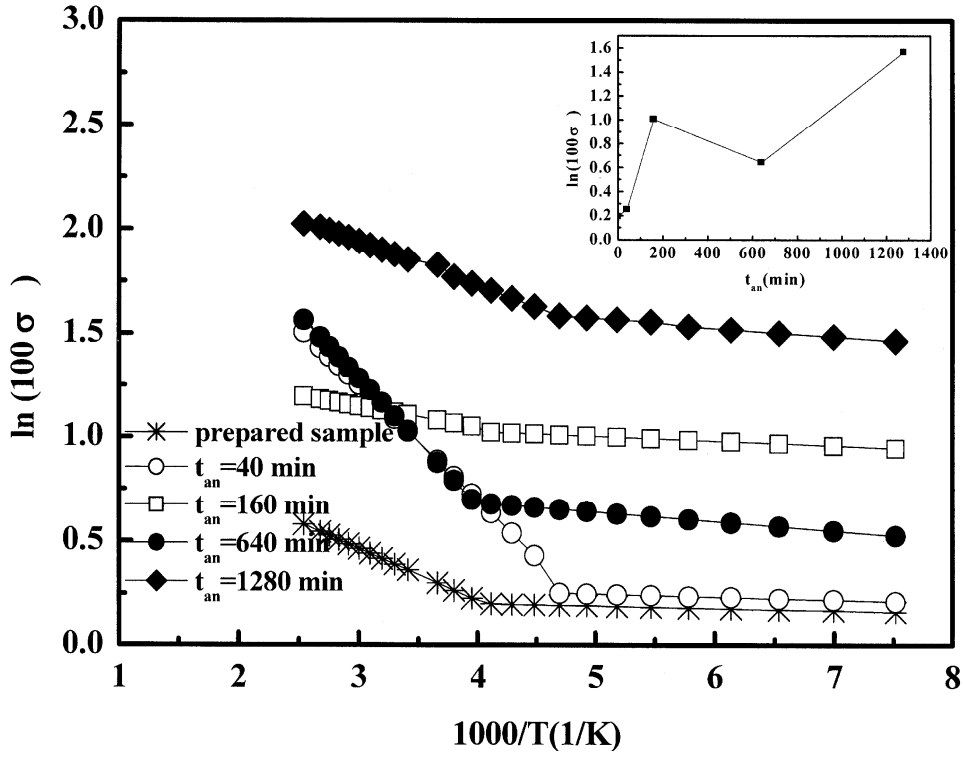

Fig. 4—Temperature dependence of conductivity at different annealing times for $Ge_{38}Sn_2Te_{60}$. The inset shows the dependence of conductivity on annealing time at T = 200°C

values of σ_0 and E_σ were obtained by the least square fits of the experimental data of Figs 3 and 4 , listed in Tables 1 and 2. In addition, the effect of the annealing time is also given in Tables 1 and 2. As it is seen in the inset in Figs 3 and 4, the annealing time dependence of σ at T= 200 K shows N-like shape with maximum value of σ at the longest annealing time and minimum value for annealing time 0 min for the prepared samples of the two compositions. For the two composition the electrical conductivity activation energy increases with transition from one stage to the second successive higher stage of σ-T dependence i.e. $E_{\sigma 1} < E_{\sigma 2}$. This indicates that the conductivity becomes more thermally activated with increasing temperature, this strengthens the prediction of dominance of hopping mechanism at the lower range of temperature.

Data in Tables 1 and 2 illustrate that for the Sn free composition, the values of both E_σ and σ_0 are dependent on annealing time. Values of both $E_{\sigma 1}$ (which corresponds to the relatively low range of T) possessed minimum at 40 min while $E_{\sigma 2}$ (which corresponds to the relatively high range of T) showed unsequential change with prolongating time of annealing with its lowest value at 160 min of annealing. Meanwhile, the general trend was that, σ_{01} increased with increasing the annealing time, while σ_{02} changed unsequentially with prolongating the time of annealing.

For the second composition, the values of E_σ and σ_0 fluctuate with prolongating the time of annealing as shown in Table 2.

As the prepared sample compositions have a polycrystalline structure indicated by XRD analysis (Figs 1 and 2), the conduction is expected to be mixed. In such a case, the measured conductivity is a sum of both extended (σ_{ext}) and hopping (σ_{hop}) components.

$$\sigma = \sigma_{ext} + \sigma_{hop} \quad \ldots (2)$$

The plots in Figs 3 and 4 were extrapolated to the lowest temperature and then σ_{hop} was determined by subtracting the values of σ (low temperature) from the measured values of σ .

The Mott's formula[13] for the temperature dependence of the hopping conductivity is

$$\sigma_{hop}\sqrt{T} = \sigma_o' \exp(-B/T^{1/4}) \quad \ldots (3)$$

where B is given by[14]

$$B = T_0^{1/4} = 2.1\left[\frac{\alpha^3}{kN(E)}\right]^{1/4} \quad \ldots (4)$$

where, σ_o' is a pre-exponent factor, α describes the spatial extent of the localized wave function, which was assumed to be 0.1 Å^{-1} and $N(E)$ is the density of the localized states (DOLS) at the Fermi level.

Table 1—Variation of E_σ(eV) , σ_o(Ω.cm)$^{-1}$(the extrapolation to T^{-1} =0 at both the low and the high temperature regions of conduction), and T_r (K) (the temperature of transition from the hopping to the extended state conduction ranges) with time of annealing for $Ge_{40}Te_{60}$

t_{an}(mins)	$E_{\sigma 1}$(eV)	σ_{o1}(Ω.cm)$^{-1}$	$E_{\sigma 2}$(eV)	σ_{o2}(Ω.cm)$^{-1}$	T_r(K)
0	1.636×10^{-3}	0.013	63.3×10^{-3}	0.234	243
40	0.11×10^{-3}	0.018	8.84×10^{-3}	0.029	223
160	1.07×10^{-3}	0.018	4.41×10^{-3}	0.021	233
640	2.34×10^{-3}	0.017	50.93×10^{-3}	0.153	243
1280	2.97×10^{-3}	0.031	29.47×10^{-3}	0.109	233

Table 2—Variation of E_σ(eV) , σ_o(Ω.cm)$^{-1}$(the extrapolation to T^{-1} =0 at both the low and the high temperature regions of conduction), and T_r (K) (the temperature of transition from the hopping to the extended state conduction ranges) with time of annealing for $Ge_{38}Sn_2Te_{60}$

t_{an}(mins)	$E_{\sigma 1}$	σ_{o1}(Ω.cm)$^{-1}$	$E_{\sigma 2}$	σ_{o2}(Ω.cm)$^{-1}$	T_r
0	0.95×10^{-3}	0.013	21.40×10^{-3}	0.034	223
40	1.30×10^{-3}	0.014	47.76×10^{-3}	0.185	223
160	1.94×10^{-3}	0.031	8.79×10^{-3}	0.043	243
640	3.50×10^{-3}	0.024	52.93×10^{-3}	0.228	243
1280	3.41×10^{-3}	0.058	19.50×10^{-3}	0.135	243

The straight line fits shown in Figs 5 and 6 confirm that the conductivity data in the range below 260 K satisfy Mott's formula and can be used to calculate $N(E)$ and consequently to calculate the basic parameters characterizing variable-range hopping (VRH) conduction namely[13], the hopping distance(R_h)

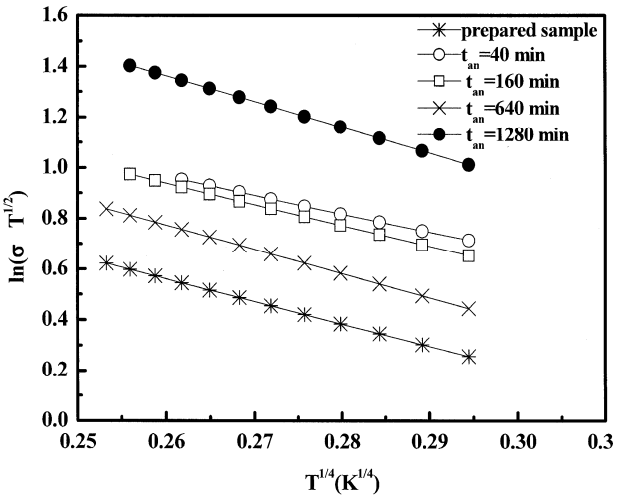

Fig. 5—The relation between ln $(\sigma T^{1/2})$ and $T^{1/4}$ for $Ge_{40}Te_{60}$ at different times of annealing

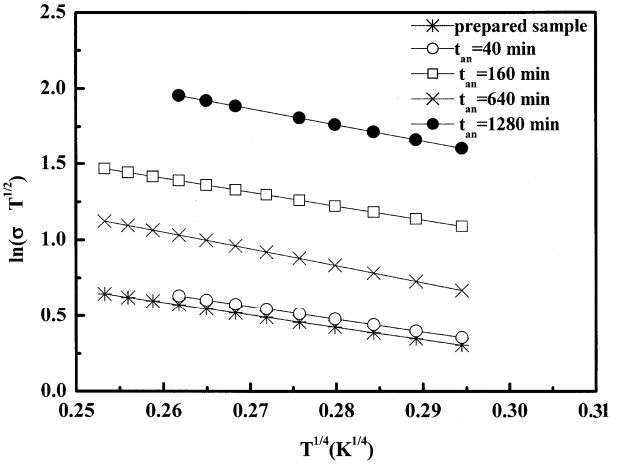

Fig. 6—The relation between ln $(\sigma T^{1/2})$ and $T^{1/4}$ for $Ge_{38}Sn_2Te_{60}$ at different times of annealing

and the hopping energy (W) which are given, respectively, as

$$R_h = \left(\frac{9}{8\pi\alpha N(E)kT}\right)^{1/4} \quad \ldots (5)$$

$$W = \frac{3}{4\pi R_n^3 N(E)} = \left(\frac{2\alpha^3 k^3 T^3}{9\pi N(E)}\right)^{1/4} \quad \ldots (6)$$

The calculated values of $N(E)$, R_h and W for the two compositions are listed in Table 3. The values of $N(E)$ is the maximum at t_{an} = 40 min for $Ge_{40}Te_{60}$ and at t_{an}= 0 min for $Ge_{38}Sn_2Te_{60}$ and both R_h and W had a minimum at t_{an}= 40 min for $Ge_{40}Te_{60}$.

For the $Ge_{38}Sn_2Te_{60}$, $N(E)$ attained a maximum before annealing, while both R_h and W have minimum values. Moreover, for the two considered compositions, the values of $N(E)$ are unreasonably high compared to those recorded previously[15,16] for Ge alloys. This indicates that hopping may be the only dominant mechanism contributing to the conduction process in the compositions.

As it is seen in Figs 7 and 8 the plots between Seebeck coefficient (S) and $1/T$ in the same temperature range mentioned before for different

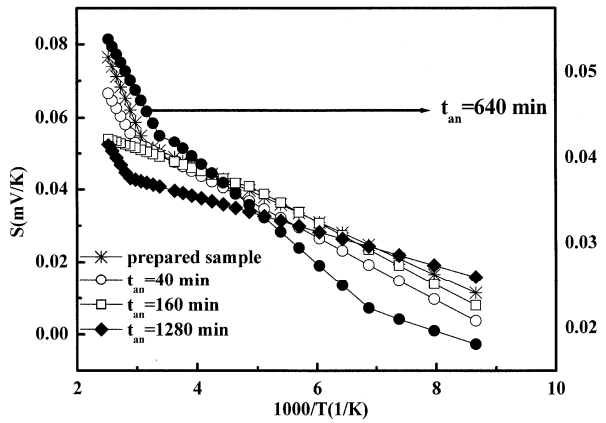

Fig. 7—The relation between Seebeck coefficient and 1000/ T for $Ge_{40}Te_{60}$ at different times of annealing

Table 3—Variation of $N(E)$ (cm^{-3} eV^{-1}), R_h (nm), and $W(eV)$ with time of annealing (minutes)

t_{an}(minutes)	$Ge_{40}Te_{60}$			$Ge_{38}Sn_2Te_{60}$		
	$N(E)$	R_h(nm)	W(eV)	$N(E)$	R_h(nm)	W(eV)
0	3.84×10^{21}	1.378	0.0237	5.2×10^{21}	1.277	0.0220
40	8.330×10^{21}	1.136	0.0196	4.7×10^{21}	1.312	0.0225
160	4.99×10^{21}	1.292	0.0222	3.4×10^{21}	1.422	0.0245
640	2.88×10^{21}	1.480	0.0256	1.6×10^{21}	1.708	0.0294
1280	2.241×10^{21}	1.58	0.0270	1.9×10^{21}	1.646	0.0284

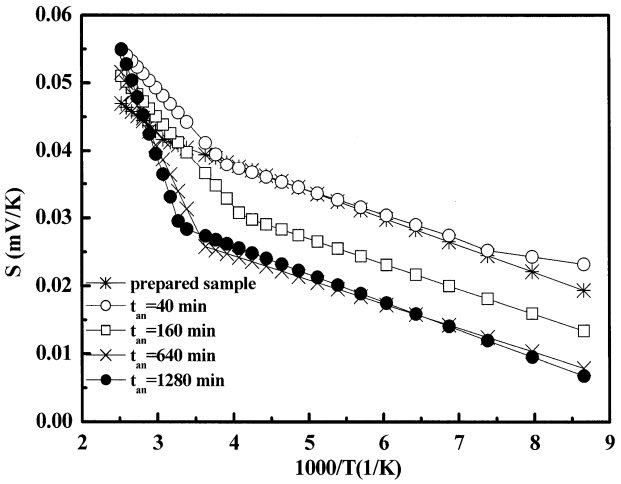

Fig. 8—The relation between Seebeck coefficient and 1000/ T for $Ge_{38}Sn_2Te_{60}$ at different times of annealing

annealing times (t_{an}= 0, 40, 160, 640 and 1280 min) are kinked linear. Accordingly, the temperature dependence of the differential thermoelectric power can be described by the following relation:

$$S = \pm \frac{k}{e}\left(\frac{E_s}{kT} + A'\right) \quad \ldots (7)$$

where the plus and minus sign are for p-type and n-type materials, respectively. E_s represents the Fermi energy[17,18] (chemical potential). A' is a dimensionless parameter concerned with the carriers scattering mechanism[19] or assumed to be a measure of the kinetic energy transported by carriers[20]. The samples at all considered annealing times exhibited negative sign TEP proving that these materials are of n-type. The electrons contributing to the observed TEP showed thermal activation and thus, the value of S increases continuously with increasing T. However, such thermal activation of electrons becomes more stronger as the temperature increase depends on the time of annealing. The relation between S and $\frac{1}{T}$ can be devided into two parts for all times of the two figures except for t_{an} = 640 min and t_{an} = 40 min for $Ge_{40}Te_{60}$ and $Ge_{38}Sn_2Te_{60}$, respectively. At low range of temperature (first part), the contribution of holes to the observed thermoelectric power seemed very significant for t_{an}= 640 min and t_{an}= 40 min for $Ge_{40}Te_{60}$ and $Ge_{38}Sn_2Te_{60}$, respectively, as almost entire compensation of the different sign contributing charge carriers could be observed at t_{an}= 640 min and t_{an}= 40 min, respectively.

Besides, values of the activation energy in the range below E_{s1} and above E_{s2}, the knee temperature (T_r) and the dimensionless parameter A_1' and A_2' corresponding to the extraploation of the ranges below and above T_r, vary with annealing time as shown in Tables 4 and 5.

As it is seen, the value of E_{s1} is in general small, this reflects the possibility of mixed conduction. Besides, $E_{s1} < E_{s2}$, which emphasizes that the contribution of electrons becomes more dominant in the relatively high range of temperature, the values of E_{s1} for t_{an} = 640 min for $Ge_{40}Te_{60}$ and t_{an} = 40 min for $Ge_{38}Sn_2Te_{60}$ are comparatively small with respect to those for other times of annealing indicating more significant contribution of holes at these times of

Table 4—Variation of E_s(eV) , A' and T_r(K) with time of annealing (minutes) for $Ge_{40}Te_{60}$

t_{an}(mins)	E_{s1}(eV)	A_1'	E_{s2}(eV)	A_2'	T_{r1}(K)	E_{s3}(eV)	A_3'	T_{r2} (K)
0	7.45×10^{-3}	7.60×10^{-2}	39.3×10^{-3}	17.6×10^{-2}	315.5			
40	8.71×10^{-3}	7.92×10^{-2}	29.6×10^{-3}	14.2×10^{-2}	325.5			
160	8.66×10^{-3}	8.3×10^{-2}	5.85×10^{-3}	6.89×10^{-2}	205.5			
640	2.28×10^{-3}	3.79×10^{-2}	6.03×10^{-3}	6.38×10^{-2}	145.5	13.1×10^{-3}	8.68×10^{-2}	295
1280	4.73×10^{-3}	5.69×10^{-2}	27.1×10^{-3}	12.1×10^{-2}	355.5			

Table 5—Variation of E_s(eV) , A' and T_r(K) with time of annealing (minutes) for $Ge_{38}Sn_2Te_{60}$

t_{an}(mins)	E_{s1}(eV)	A_1'	E_{s2}(eV)	A_2'	T_{r1}(K)	E_{s3}(eV)	A_3'	T_{r2}(K)
0	3.9910^{-3}	5.39×10^{-2}	8.9710^{-3}	6.97×10^{-2}	325.5			
40	1.5810^{-3}	3.69×10^{-2}	3.5410^{-3}	5.17×10^{-2}	145.5	12.510^{-3}	8.64×10^{-2}	265.5
160	3.710^{-3}	4.55×10^{-2}	13.1310^{-3}	8.42×10^{-2}	245.5			
640	3.610^{-3}	3.87×10^{-2}	23.6810^{-3}	11.14	245.5			
1280	4.0910^{-3}	4.22×10^{-2}	34.2010^{-3}	14.15×10^{-2}	305.5			

annealing. The corresponding relatively small values obtained for A' as seen in Tables 4 and 5 is a strong confirmation of mixed conduction behaviour.

Refering to the data in Tables 1-4, the variation of both E_σ and E_s with the time of annealing is similar.

This can be explained on the basis that addition of Sn has small effect on the internal microstructure. Furthermore, the unsequential variation in E_σ and E_s can reflect unsequential variation of the internal microstructure of both compositions with prolongating the time of annealing.

The difference between E_σ and E_s for two compositions confirms that hopping conduction can be dominant especially in the low temperature range.

4 Conclusion

The X-ray diffractogram patterns showed that the method of preparation is successful for obtaining $Ge_{40}Te_{60}$ and $Ge_{38}Sn_2Te_{60}$ as dominant phases in the compositions. The σ -T dependence emphasized the semiconductor behaviour of both compositions. Their electrical conduction is via the extended states in the higher range of temperature and is that of localized states in lower range of temperature. Morever, the effect of the annealing time on E_σ may be controlled by two opposite (enhancing and inhibiting) factors. The S-T relation showed that S has negative sign indicating that the two compositions are of n-type behaviour. The values of E_s determined for all considered annealing times ranged from ~ 1.5 to 40 meV.

Acknowledgement

We would like to thank Prof Dr M M Ibrahiem for continuous encouragement and stimulating discussions.

References

1 Hicks L D, Harman T C, Sun X & Dresselhaus M S, *Phys Rev,* B10 (1996) 493.
2 Kan Hachiya, *J Non-Cryst Solids,* 291(2001)160.
3 Okoye C M I, *J Phys:Condens Matter,* 14 (2002) 8625.
4 Haruvi-Busnach I, Dror J & Croitoru N, *J Matter Res,* V.5 N. 6 (1996) 1215.
5 Lippens P E, Aldon L, Olivier-Fourcade J, Jumas J C, Gheorghiu de la Rocque A & Sènèmaud C, *J Phys & Chem Solids*, 60 (1999) 1745.
6 Delin Anna, Ravindran P, Erickson P & Olle Wills J M, *Int J Quantum Chem,* 69 (1998) 349.
7 Rabe K M & Joannopoulos J D, *Phys Rev B,* 32 (1985) 2302.
8 Rabii S, *Phys Rev,* 182 (1969) 821.
9 Rabii S, *Bull Am Phys Soc,* 13 (1968) 413.
10 Mkorn D & Braunstein R, *Phys Rev B,* 5 (1972) 4837.
11 Suziki N & Adachi S, *Japan J Appl Phys,* 34 (1995) 5977.
12 Cardona M & Greenaway D L, *Phys Rev A,* 133 (1964) 1685.
13 Mott N F & Davis E A, *Electronic processes in non-crystalline materials,* [Clarendon Press, Oxford] (1979).
14 Chaudhuri B K, Chaudhuri K & Som K K, *J Phys & Chem Solids,* 50 (1989) 1149.
15 Ibrahiem M M, Ahmed A M & Megahid N M, *Indian J Pure & Appl Phys,* 34 (1996) 172.
16 Giridhar A, Narasikham P S L & Mahadevan S, *J Non-Cryst Solids,* 37 (1980)165.
17 Edmond J T, *Br J Appl Phys*, 17 (1966) 979.
18 Culter M & Mott N F, *Phys Rev*, 181 (1969) 1336.
19 Mott N F & Davis E A, *Electronics in Non-Crystalline Materials* (Clarendon Press, Oxford) (1977) 217.
20 Loffe A F, *Physics of Semiconductors* (Info Search, London), (1960) 288, Heikes R & Ure R W (Jr), *Thermoelectricity, Science and Engineering* (Interscience. New York), 1961; Tauc J, *Photo and thermoelectric effects in semiconductors* (Pergamon, New York) 1962.